

The vanadate-tolerant yeast *Hansenula polymorpha* undergoes cellular reorganization during growth in, and recovery from, the presence of vanadate

Ilaria Mannazzu, Emanuela Guerra, Rosanna Strabbioli, Dario Pediconi and Fabrizio Fatichenti

Author for correspondence: Ilaria Mannazzu. Tel: +39 71 2204855. Fax: +39 71 2204858.
e-mail: ilaria@popcsi.unian.it

Dipartimento di
Biotecnologie Agrarie ed
Ambientali, Università di
Ancona, Via Brecce
Bianche, Ancona 60131,
Italy

When present at intracellular concentrations above micromolar, vanadate becomes toxic to most organisms. However, the yeast *Hansenula polymorpha* is able to grow on vanadate concentrations in the millimolar range, showing at the same time modifications in cellular ultrastructure and polyphosphate metabolism. Here, the development of the ultrastructural changes, and of vacuolar and secretory activities, during exponential growth on vanadate and upon a return to vanadate-free conditions was investigated. External invertase secretion was inhibited by vanadate, as shown by a decrease in external invertase activity, an intracellular accumulation of small vesicles and a cytoplasmic accumulation of internal invertase. An aberrant appearance of the cell wall and defects in cellular surface growth, possibly linked to defects in secretion, were also observed. However, inhibition of the secretory pathway was not complete since the activity of another secreted enzyme, exoglucanase, increased in the presence of vanadate. Growth on vanadate was also accompanied by an enhancement of vacuolar proteolysis, as indicated by an increase in carboxypeptidase Y activity. However, these modifications were all reversible upon return to vanadate-free conditions, with the normalization process being complex and involving new and dramatic ultrastructural changes and activation of an autophagic mechanism. This mechanism is involved in the elimination/resorption of the observed vanadate-induced aberrant cell structures and/or sites involved in vanadate accumulation, a necessary prerequisite for restoration of conventional ultrastructure and metabolic functions.

Keywords: *Hansenula polymorpha*, vanadate, ultrastructure, secretion, vacuolar activity

INTRODUCTION

It has been reported that the addition of vanadate (VO_4^{3-}) to the whole-cell system, in which vanadate can be reduced to vanadyl (VO^{2+}), increases DNA synthesis (Smith, 1983), protein phosphorylation (Brown & Gordon, 1984; Karlund, 1985), chloride transport (Hatch *et al.*, 1983) and cAMP levels (Catalan *et al.*, 1980), and has an insulin-mimetic effect (Crans *et al.*, 1995). Furthermore, *in vivo* and *in vitro* studies have

shown an inhibitory effect of vanadate on Na^+/K^+ and P-type ATPases (Cantley *et al.*, 1978; Karlsh *et al.*, 1979; Wach & Graber, 1991), RNases (Lindquist *et al.*, 1973), protein-acid- and alkaline phosphatases (Foulkes *et al.*, 1983), phosphofructokinase and adenylate kinase (Chasteen, 1984). However, the mechanisms by which vanadium exerts a toxic effect on living organisms are not completely understood. This could be due to the variety of possible intracellular targets of the metal and to the changes in chemical form and oxidation state that vanadium can undergo (for details see Willsky, 1990) both in the external environment and intracellularly.

Whilst little is known about the apparent stimulatory

Abbreviations: CPY, carboxypeptidase Y; ExG, exoglucanase; ExI, external invertase; TEM, transmission electron microscopy.

effect of vanadyl on metabolic processes, a mechanism of 'ionic mimicry' seems to be responsible for many of the effects of vanadate. Vanadate has structural and metabolic similarities with phosphate: it enters the cell through the phosphate transport system in erythrocytes (Cantley *et al.*, 1978), *Neurospora crassa* (Bowman, 1983) and *Saccharomyces cerevisiae* (Willsky *et al.*, 1984) and affects many metabolic circuits by competing with endogenous phosphate in enzymic- and receptor-mediated processes.

In the yeast *S. cerevisiae* a detoxifying mechanism that can work efficiently at low vanadate concentrations has been hypothesized. In this case, after entering the cell, vanadate is reduced to vanadyl and then excreted in this form. However, at higher concentrations, the rate of vanadate influx overtakes that of vanadate reduction. Consequently, vanadate accumulates intracellularly, leading to the formation of toxic high-molecular-mass vanadate compounds which stop growth (Willsky *et al.*, 1984). *S. cerevisiae* vanadate-resistant mutants do not accumulate vanadate compounds intracellularly and exhibit several phenotypic modifications, such as plasma membrane and cell wall aberrations, underglycosylation of secreted invertase, sporulation defects and increased sensitivity to hygromycin and detergents (Ballou *et al.*, 1991; Kanik-Ennulat *et al.*, 1995). All the genes implicated in vanadate resistance isolated so far code for proteins involved in the organization and functioning of the Golgi apparatus and the secretory pathway. Different models have been hypothesized for this resistance. Ballou *et al.* (1991) proposed that any mutation of a vanadate-sensitive target site involved in protein sorting in the Golgi, or in vanadate uptake, secretion or detoxification, could be responsible for vanadate resistance. Kanik-Ennulat *et al.* (1995) suggested that vanadate resistance could arise from alterations in the secretory pathway, which would allow cells to dilute or excrete toxic vanadate molecules formed intracellularly. These authors hypothesized that either a proliferation of the Golgi apparatus or a modification of vesicle or membrane targeting at the level of the Golgi could be responsible for the decreased toxicity of vanadate and for the general plasma membrane and cell wall defects observed in the vanadate-resistant mutants.

In the vanadate-tolerant yeast *Hansenula polymorpha*, growth in the presence of vanadate induces changes in cellular ultrastructure and in polyphosphate metabolism, and the appearance of intracellular vanadyl; such effects could indicate the activation of a detoxifying mechanism (Mannazzu *et al.*, 1997). To understand the role of the observed modifications in vanadate tolerance, we have investigated the development of ultrastructural changes and of vacuolar and secretory activities during exponential growth on vanadate and upon return to vanadate-free conditions.

METHODS

Growth conditions. *H. polymorpha* strain NCYC 495 was used. Media used were GYNB (2% glucose, 0.7% Difco Yeast Nitrogen Base without amino acids), VGYNB (GYNB plus

50 mM sodium orthovanadate), SYNB (2% sucrose, 0.7% Difco Yeast Nitrogen Base without amino acids) and VSYNB (SYNB plus 50 mM sodium orthovanadate), all at pH 5.8. Sodium orthovanadate (Sigma) was added to the sterile medium from a filter-sterilized stock solution (500 mM, pH 5.8). Unless otherwise stated, 1×10^6 cells ml⁻¹ from overnight precultures in GYNB were used as inoculum. Cells were grown aerobically at 37 °C in an orbital shaker (240 r.p.m.).

Growth assessment. For growth rate calculations, growth was followed by measuring the OD₆₀₀ every 2 h (Cary 1E UV-Vis, Varian spectrophotometer) using the supernatant as blank. For experiments on sucrose utilization and recovery from vanadate, growth was measured by cell counting in a haemocytometer.

Recovery from vanadate. Cells grown to mid-exponential phase on VGYNB or GYNB were harvested by centrifugation, washed twice in water and reinoculated into GYNB to a final concentration of 2.5×10^7 cells ml⁻¹. Samples for growth assessment and ultrastructural and enzymic analyses were taken immediately after transfer to GYNB (time zero) and after a further 30, 60, 120 and 240 min.

Ultrastructural analyses. Cells were harvested by centrifugation, washed three times in water and fixed in 1% potassium permanganate for 20 min at room temperature. Pellets were then dehydrated in a graded series of ethanol concentrations (15 min for each solution containing 25, 60, 80 and 95% ethanol), embedded in Epon Araldite overnight at room temperature and treated at 60 °C for 24 h. Ultrathin sections of the order of 50 nm in thickness were stained for 40 s in a solution of lead citrate and observed by transmission electron microscopy (TEM; Philips CM12 electron microscope operating at 80 kV). For the ultrastructural analyses, 20–60 cells for each sample were selected at random and photographed at a final magnification of $\times 40000$. Relative vacuolar volumes were estimated using a stereological method according to Weibel (1979). Vesicles were scored as electron-dense disks or rings 35–45 nm in diameter. Vesicle counts were normalized for cell volume, which was calculated by measuring the area of the cell section (measured from the plasma membrane) and using a section thickness of 50 nm.

Immunoelectron microscopy. Cell fixation was performed as described by Mulholland *et al.* (1994), modified as follows. A 20 ml volume of a culture of cells growing exponentially (2.5×10^7 cells ml⁻¹) on GYNB and VGYNB were harvested by filtration through a 0.45 µm pore-size nitrocellulose filter. Cells were dehydrated in a graded series of ethanol concentrations (5 min on ice for each solution containing 30, 80, 95 and 100% ethanol) and embedded in LR White embedding resin (Electron Microscopy Sciences), which was then polymerized. Ultrathin sections (40–50 nm) were mounted on nickel grids and immunolabelled according to the method of Preuss *et al.* (1991). Anti-invertase antibody (kindly provided by Dr Jesus Zueco, Universidad de Valencia, Spain) was diluted 1:100 in PBST (140 mM NaCl, 3 mM KCl, 8 mM Na₂HPO₄, 1.5 mM KH₂PO₄, 0.05% Tween 20) containing 0.5% BSA and 0.5% ovalbumin. EM goat antirabbit IgG secondary antibody conjugated to 10 nm diameter gold particles (British BioCell International) was diluted 1:50 in PBST. Observations were made using a Philips CM12 electron microscope operating at 120 kV.

Enzymic assays. External invertase (ExI) activity was assayed on whole cells as described by Goldstein & Lampen (1975), modified as follows. The enzymic and colorimetric reactions were carried out at 37 °C for 10 min and 20 min, respectively;

the enzymic reaction was stopped by the addition of 0.3 ml 0.2 M K_2HPO_4 pH 10; the colorimetric reaction was stopped by the addition of 2 ml 6M HCl. One unit (U) corresponds to 1 μ mol glucose released min^{-1} and activity is expressed as U (mg dry wt) $^{-1}$. Total invertase (external plus internal) was assayed on crude extracts as described above. Activity is expressed as U (mg protein) $^{-1}$.

Exoglucanase (ExG) activity was determined on whole cells as described by Santos *et al.* (1979), modified as follows. The enzymic reaction was carried out in 0.25 ml buffer containing 0.25% *p*-nitrophenyl- β -D-glucopyranoside as substrate, 50 mM acetate buffer pH 5.5, 10 mM NaN_3 , 0.1% Triton X-200, and incubated at 37 °C for 3 h. The concentration of *p*-nitrophenol was measured by adding 2 ml of 4% Na_2CO_3 to 0.25 ml of the reaction mixture. One unit (U) corresponds to 1 nmol *p*-nitrophenol released min^{-1} and activity is expressed as U (mg dry wt) $^{-1}$.

Carboxypeptidase Y (CPY) activity was assayed on crude extracts according to a modification of the method of Aibara *et al.* (1971). Briefly, 0.1 ml 6 mM *N*-benzoyl-L-tyrosine-*p*-nitroanilide (BTPNA; Sigma) in dimethylformamide was added to 0.4 ml 0.1 M Tris/HCl pH 7.6 and 0.1 ml crude extract at 37 °C. After 30 min, 1.5 ml 1 mM $HgCl_2$ was added to stop the reaction, followed by addition of 0.2 ml 20% SDS and 3 min incubation at 60 °C to solubilize proteins. After 10 min at room temperature, the absorbance at 410 nm was determined (Cary 1E UV-Vis, Varian spectrophotometer). One unit (U) corresponds to 1 μ mol *p*-nitroaniline produced min^{-1} (molar absorption coefficient of *p*-nitroaniline = 8800 $M^{-1} cm^{-1}$). Activity is expressed as mU (mg protein) $^{-1}$.

Preparation of crude extracts. Between 0.5 and 1.0×10^9 cells were harvested by centrifugation, washed twice in water and resuspended in 0.2 ml 0.1 M Tris/HCl pH 7.6. About 0.7 vol. glass beads (diam. 45 μ m, Sigma) was added, and the cells were broken by eight cycles of 30 s vortexing interspersed with 30 s in ice. The supernatant was collected by 10 min centrifugation in a microcentrifuge. The protein concentration of the extracts was determined according to Bradford (1976), using BSA as standard.

RESULTS

Growth on vanadate induces ultrastructural and physiological modifications

Whilst we have indicated previously that there is a visible (in TEM) thickening of the cell wall and increase in the number of small cytoplasmic vesicles in *H.*

polymorpha grown on VGYNB (Mannazzu *et al.*, 1997), these studies have now been extended to demonstrate the level and significance of these effects (see Table 1). At the vanadate concentration used (50 mM), causing a 2.5-fold increase in generation time, there was also a doubling in cell wall thickness. We also observed formation of cell aggregates during growth and modifications in the cell wall matrix, such that it appeared bilayered and displayed an increased resistance to lytic enzymes (data not shown). In a small fraction of cells (4.9%) electron-dense bodies were observed embedded in the cell wall (as also illustrated in Fig. 3d; see below), which were surrounded by less electron-dense material that was not distinguishable from cell wall matrix. Their content was occasionally connected to, and could not be differentiated from, the dense peripheral cytoplasm.

Cytoplasmic vesicles of about 40 nm diameter were observed in both GYNB- and VGYNB-grown cells, but their number increased by 167% in the presence of vanadate (see Table 1). Since vanadate is known to cause an inhibition of secretory vesicle release (Lew & Simon, 1991) and an accumulation of 30–50 nm cytoplasmic vesicles has been observed in *S. cerevisiae sec* mutants (Novick *et al.*, 1980; Rambourg *et al.*, 1994), we tested the ability of *H. polymorpha* to grow on sucrose (requiring invertase secretion) in the presence of vanadate (data not shown). After 48 h the cell concentration in VSYNB cultures was more than one order of magnitude lower than that of VGYNB cultures. This was due to the presence of vanadate as control cultures (on SYNB and GYNB) grew to equal extents. However, the difference was less marked after 72 h and disappeared after 120 h, when VSYNB cultures reached the same stationary-phase cell concentration as VGYNB and control cultures. The observed behaviour seemed to indicate a partial inhibition of secretion by vanadate, which could have caused the observed increase in vesicle number when cells were grown on VGYNB. To test this hypothesis we measured the levels of two secreted enzymes, ExI and ExG, under the same culture conditions used for TEM analyses. Whilst total (external plus internal) invertase was not significantly different in GYNB- and VGYNB-grown cells (data not shown), we observed a 39% ($P < 0.001$) inhibition of ExI activity under VGYNB growth conditions (Table 1). This

Table 1. Vanadate induces ultrastructural and metabolic modifications in *H. polymorpha*

TEM analyses and measurements of growth rates and enzymic activities were performed on NCYC 495 cells growing exponentially in GYNB (control) or VGYNB, as described in Methods. Data given are means \pm SE. ExI, external invertase; ExG, exoglucanase; CPY, carboxypeptidase Y.

Conditions	Generation time (h $^{-1}$) [*]	Cell wall thickness (μ m) [†]	Small cytoplasmic vesicles [‡]		ExI activity [U (mg dry wt) $^{-1}$] [‡]	ExG activity [U (mg dry wt) $^{-1}$] [*]	CPY activity [U (mg protein) $^{-1}$] [*]
			Size (nm)	No. (μ m $^{-3}$)			
GYNB	1.413 \pm 0.033	0.101 \pm 0.004	39.40 \pm 1.90	54.61 \pm 4.36	0.115 \pm 0.004	0.104 \pm 0.003	1.213 \pm 0.037
VGYNB	4.793 \pm 0.318§	0.197 \pm 0.012§	42.10 \pm 1.72	145.87 \pm 12.62§	0.070 \pm 0.002§	0.296 \pm 0.014§	2.873 \pm 0.092§

^{*} $n = 3$. [†] $n = 50$. [‡] $n = 14$. [§] Significantly different from value for GYNB ($P < 0.001$).

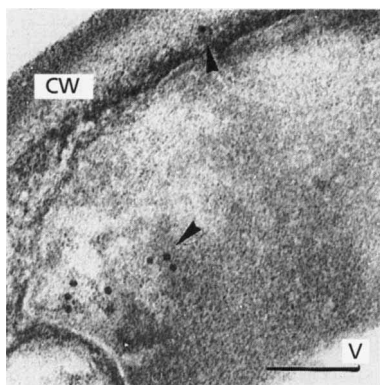


Fig. 1. Immunogold labelling of invertase in VGYNB-grown *H. polymorpha* cells. Arrowheads indicate 10 nm diameter gold particles. CW, cell wall; V, vacuole. Bar, 0.1 μm .

indicates that vanadate inhibits secretion, rather than overall production, of invertase and causes the accumulation of internal invertase. Also, by means of immunogold staining using an anti-invertase antibody, the localization of invertase was shown to be mainly cytoplasmic in VGYNB-grown cells (Fig. 1). The decrease in invertase secretion was accompanied by a 185% ($P < 0.001$) increase in ExG activity in the presence of vanadate. These results indicated a divergence in the pathway to the cell surface for the two enzymes tested and a selective inhibitory effect of vanadate on invertase secretion.

A vanadate-induced doubling in vacuolar area has previously been observed in *H. polymorpha* (Mannazzu *et al.*, 1997). To test whether the increased vacuolar area was accompanied by an increase in proteolytic activity, CPY activity was measured in cells growing exponentially with and without vanadate. As shown in Table 1, CPY activity more than doubled in the presence of the metal. Furthermore, under the same growth conditions, the majority of vacuoles contained electron-dense material. In some cells (5.1%) vacuoles also showed finger-like protrusions (see also below). This feature, previously observed in the yeast *Pichia pastoris* undergoing microautophagy under nitrogen starvation (Tuttle & Dunn, 1995), was never encountered in GYNB-grown cells.

Recovery from vanadate causes cellular rearrangements

The modifications observed during exponential growth in vanadate-containing medium were followed upon return to vanadate-free conditions. To do this, cells grown to mid-exponential phase on VGYNB were thoroughly washed and reinoculated into GYNB. At the same time, a GYNB exponential culture was similarly washed, reinoculated into GYNB and used as a control. Whereas control cultures continued to grow at the same rate, cultures transferred from VGYNB to GYNB did not show any appreciable change in cell number for the

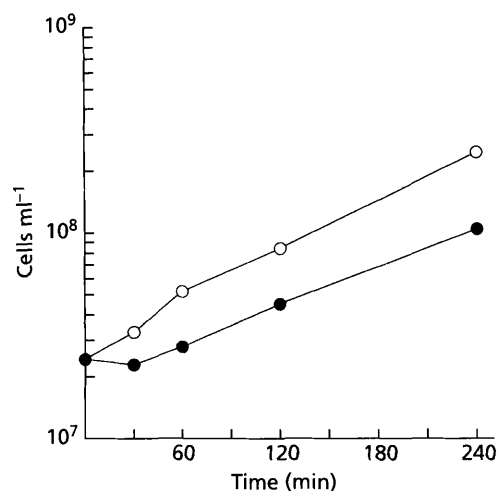


Fig. 2. *H. polymorpha* cells recovering from vanadate show a delay in growth resumption. Growth kinetics of NCYC 495 cultures grown to mid-exponential phase on GYNB (○) or VGYNB (●) and reinoculated into GYNB at a concentration of $2.0\text{--}2.5 \times 10^7$ cells ml^{-1} . Total cell numbers were counted immediately after the transfer (time zero) and after 30, 60, 120 and 240 min. The data shown are representative of five independent experiments.

first 60 min (Fig. 2), during which time cells underwent new and dramatic ultrastructural modifications (Fig. 3). Whilst immediately after the reinoculation (time zero; Fig. 3b) cells showed the typical VGYNB ultrastructure, after 30 min the percentage of cells showing vacuoles with finger-like protrusions doubled (Fig. 4a, b). Most vacuoles also contained large amounts of electron-dense material (Fig. 3c). After 60 min (Figs 3d, 4c) the electron-dense bodies sometimes observed in VGYNB-grown cells became much more evident, with an increase in the percentage of cells affected and in the number of bodies per cell (up to five). Furthermore, during this recovery phase, these electron-dense bodies could be found positioned in the cytoplasm as well as in the cell wall matrix. Whilst the appearance of both finger-like protrusions and electron-dense bodies associated with the cell wall matrix was only evident in relatively small percentages of cells under these conditions, the significance of these morphological features is supported by a consideration of their size and the thickness of the ultrathin sections (50 nm). Moreover, these features were never seen in control cells, or after the 240 min vanadate-recovery period (see below). Also, after 60 min, most vacuoles still contained large amounts of electron-dense material. At the same time, vacuolar volume showed a progressive 36% ($P < 0.001$) reduction (Fig. 4d). After 120 and 240 min, growth was resumed at a rate comparable to that of the control, and the majority of cells had an appearance increasingly similar to that of cells growing in vanadate-free medium (compare Fig. 3a with Fig. 3e and f). The plasma membrane, which appears irregular during growth on vanadate (Mannazzu *et al.*, 1997), showed a smoother contour and there was a decrease in cell wall thickness,

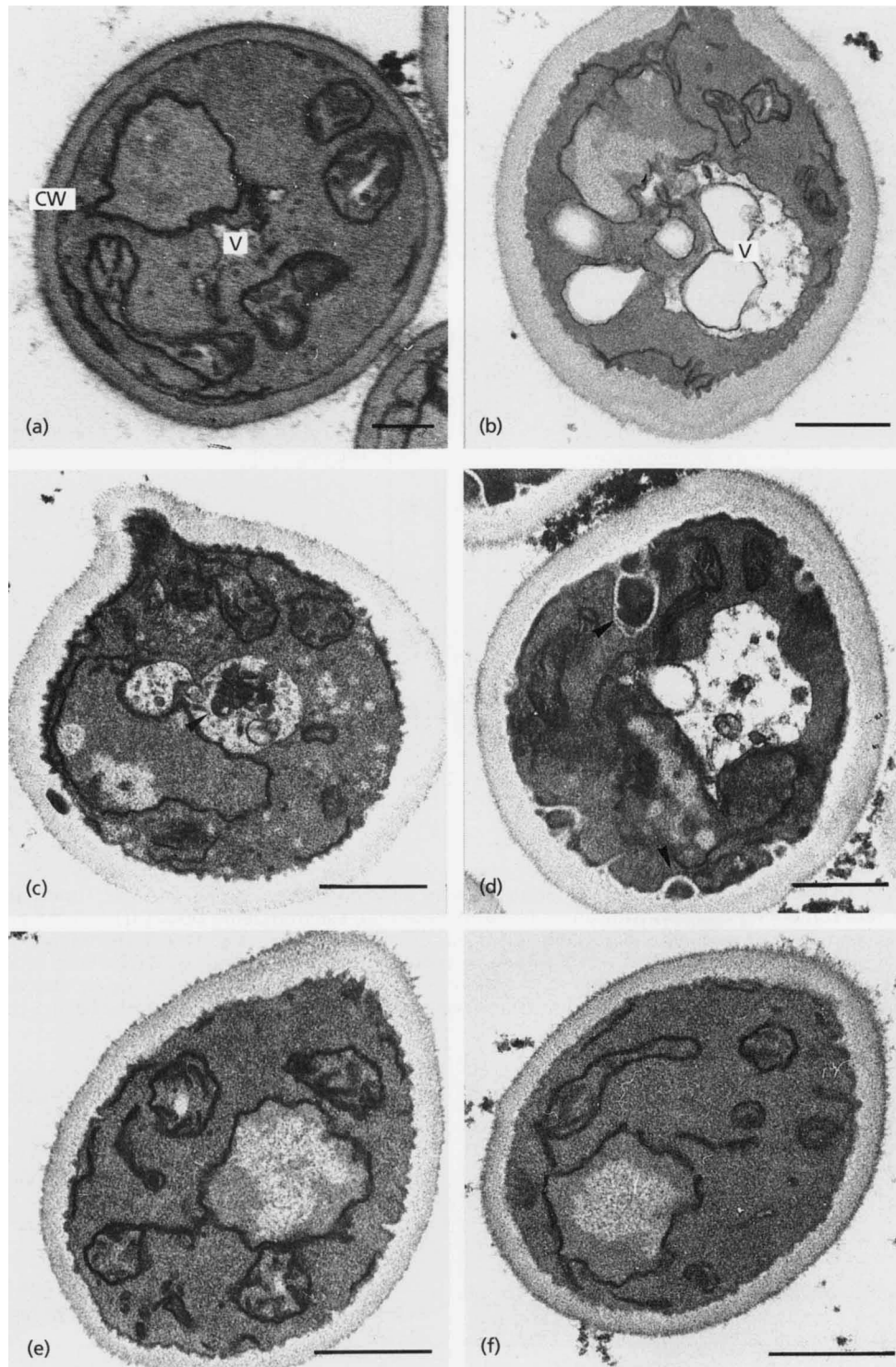


Fig. 3. Recovery of *H. polymorpha* from vanadate involves complex ultrastructural reorganization. NCYC 495 cells were grown to mid-exponential phase in VGYNB and reinoculated into GYNB at a concentration of $2.0\text{--}2.5 \times 10^7$ cells ml^{-1} . Samples were taken immediately after the transfer (b) and after 30 (c), 60 (d), 120 (e) and 240 (f) min, fixed in potassium permanganate and visualized by TEM. A similar image of NCYC 495 cells growing exponentially in GYNB (no vanadate treatment) is shown in (a) for comparison. CW, cell wall; V, vacuole; arrowheads indicate the electron-dense material inside the vacuoles and the dense structures embedded in the cell wall and in the cytoplasm. Bars, $0.5 \mu\text{m}$.

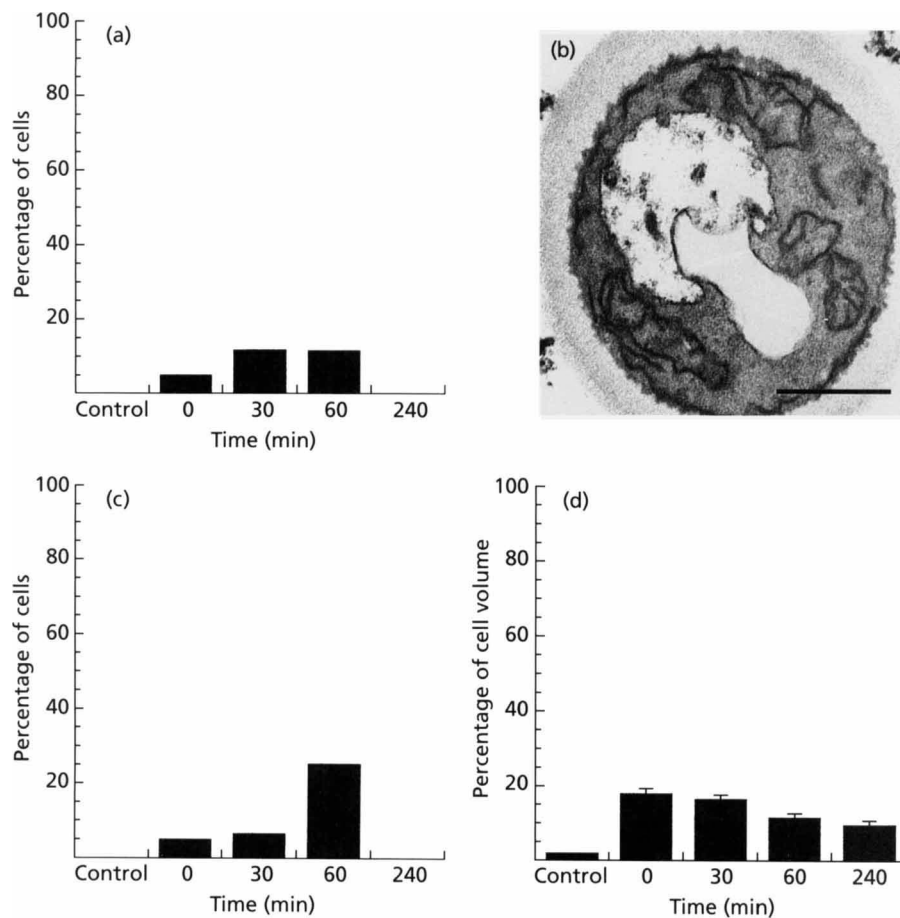


Fig. 4. Analyses of ultrastructural modifications during recovery of *H. polymorpha* from vanadate. Histograms show the percentage of cells containing vacuoles with finger-like protrusions (a), electron-dense bodies (c) and the percentage of cellular volume occupied by vacuoles (d) at the indicated times during recovery. One hundred per cent cellular volume = $1.85 (\pm 0.12 \text{ SE}) \mu\text{m}^3$. The control was a culture of cells growing exponentially in GYNB. Sixty cells selected at random were examined for each sample. Bars in (d) represent $\pm \text{SE}$. Data are representative of two independent recovery experiments. (b) TEM visualization of finger-like protrusion seen after 30 min of vanadate recovery. Bar, $0.5 \mu\text{m}$.

which at 240 min was equal to $0.109 \pm 0.004 \mu\text{m}$, not significantly different from that of the control (see Table 1 for comparison). The vacuolar volume further decreased, although it did not reach control values by 240 min (Fig. 4d).

After transfer from VGYNB to GYNB, there was also a delayed increase in ExI activity, which showed a 50% recovery in the first 60 min, thus approaching that of the control (Fig. 5a). This delayed recovery was also seen in the case of vesicle numbers (Fig. 5b), where there was an initial (30 min) increase, which was followed (after 60 min) by a gradual return to control vesicle numbers (see also Table 1). ExG activity reached a peak 60 min after reinoculation into GYNB and progressively decreased at 120 and 240 min from reinoculation (Fig. 5c), indicating that the amount of secreted ExG increased during the delay in growth resumption (see Fig. 2) and declined concomitantly with growth rate recovery. This behaviour is somewhat surprising given that ExG activity has been directly related to growth rate in *Candida albicans* (Chambers & Sullivan, 1993).

Cells transferred to vanadate-free medium also showed an initial further increase in CPY activity (Fig. 5d), which reached a peak 60 min after vanadate removal. After this time it progressively decreased, and was similar to that of the control after the 240 min recovery period. Interestingly, this higher CPY activity was concomitant with the increase in the percentage of cells containing vacuoles with large finger-like protrusions and the above-mentioned electron-dense bodies (See Fig. 4a, c).

DISCUSSION

In this report we describe some aspects of the *H. polymorpha* response to the presence of high vanadate concentrations in the growth medium and demonstrate the reversible nature of these modifications. However, the processes leading to this normalization, activated upon the return to vanadate-free conditions, are very complex and involve profound ultrastructural and metabolic rearrangements which are particularly intense

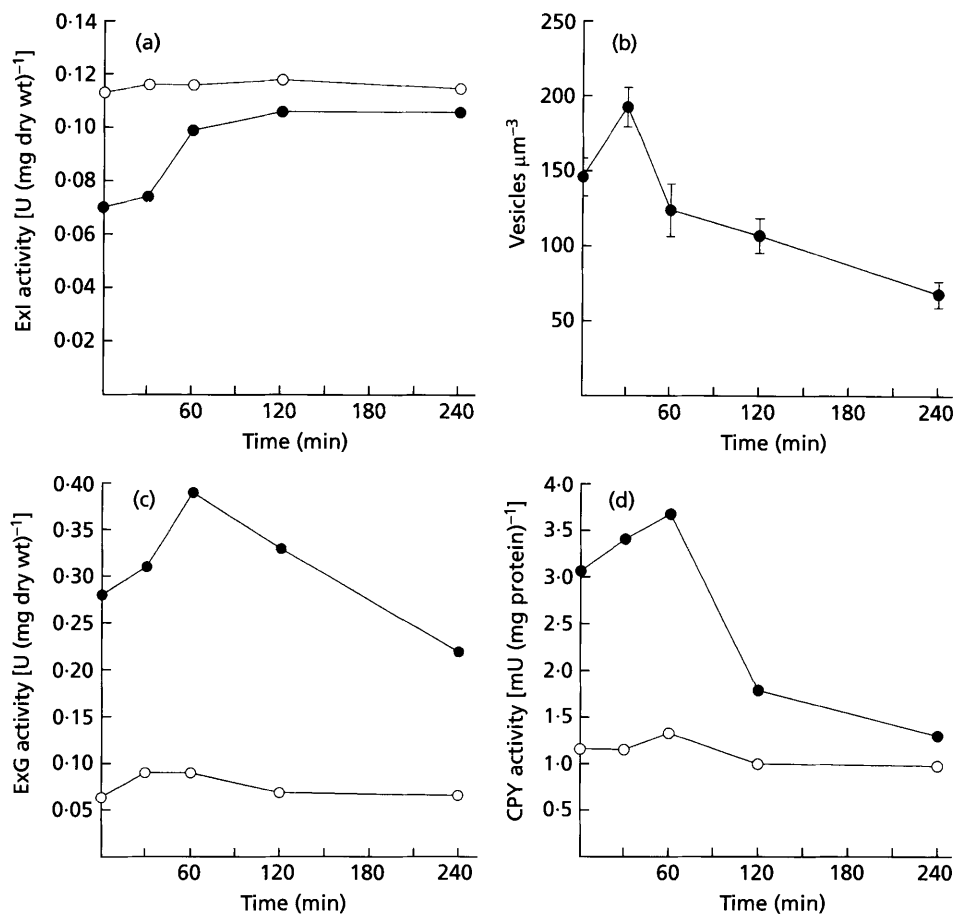


Fig. 5. *H. polymorpha* cells recovering from vanadate undergo changes in secretory and vacuolar proteolytic activities. (a) ExI activity, (b) vesicle number, (c) ExG activity and (d) CPY activity of cells transferred from GYNB (○; controls) and VGYNB (●) to GYNB. Cell samples were taken at the times indicated and assayed for enzymic activities as described in Methods. The data shown are representative of five independent experiments. Numbers of 40 nm vesicles were counted on TEM images of cells transferred from VGYNB to GYNB immediately after the transfer (time zero) and after 30, 60, 120 and 240 min. Twenty cells selected at random were examined for each sample. Bars in (b) represent \pm SE.

during the first 60 min following the transfer from VGYNB to GYNB.

The decreased growth rate in VSYNB and the accumulation of 40 nm diameter vesicles, together with the mainly cytoplasmic localization of invertase and the inhibition of ExI activity, suggest a perturbation of secretion caused by vanadate in *H. polymorpha*. The decrease in the number of cytoplasmic vesicles and the increase in ExI activity observed upon return to vanadate-free conditions are consistent with this hypothesis. Similar behaviour has also been observed in *S. cerevisiae sec* mutants, which at the non-permissive temperature do not export invertase and accumulate 50 nm secretory vesicles in the cytoplasm; upon the return to the permissive temperature, these secretory vesicles are released and ExI activity increases (Novick *et al.*, 1980). In this study, under VGYNB culture conditions, decrease in ExI activity is accompanied by an increase in CPY and ExG activities. In the case of CPY, the endoplasmic reticulum precursor p1CPY is

converted to p2CPY in the Golgi and subsequently transported to the vacuole from a late Golgi compartment. In the vacuole, p2CPY is processed to the active mature form of CPY (Mulholland *et al.*, 1997). The increased CPY activity observed in vanadate-growing cells thus indicates that protein traffic from the endoplasmic reticulum to the Golgi, as well as through the late Golgi compartment, is fully active in the presence of vanadate. Furthermore, the increased ExG activity indicates an efficient delivery of this secreted protein from the late Golgi to the cell surface under VGYNB culture conditions. Study of post-Golgi vesicles of *S. cerevisiae* mutants blocked in Golgi to cell-surface transport led Harsay & Bretscher (1995) to suggest that ExI and the major ExG normally secreted from the cell travel together from the trans-Golgi to the cell surface inside a population of secretory vesicles containing periplasmic enzymes and several plasma membrane permeases. However, an exoglucanasic activity was also found associated with a different secretory vesicle population. The vanadate-induced decrease in ExI

activity, together with the increase in ExG activity, demonstrate that, in *H. polymorpha*, these two enzymes can be exported through different pathways from late Golgi to the cell surface. This could be due to protein sorting into different vesicles from the same compartment. It has also been hypothesized that different proteins might be transported inside vesicles budding from different compartments (Harsay & Bretscher, 1995). This implies that a portion of secreted proteins could by-pass a post-Golgi intermediate compartment or a late-Golgi compartment and go to the plasma membrane through a different route. This hypothesis is supported by the results obtained by Ballou *et al.* (1991), who observed that some *S. cerevisiae* vanadate-resistant mutants show a defective glycosylation pattern of only a subset of secreted proteins, suggesting that different proteins may be processed through different glycosylation compartments. Therefore we can hypothesize the existence of a vanadate-sensitive target in the invertase route to the plasma membrane, which would not affect cellular components travelling within different secretory cargoes.

Cell wall modifications similar to those described in *H. polymorpha* growing exponentially on vanadate-containing medium have previously been observed in yeast. A heterogeneous and bilayered cell wall has been described in *S. cerevisiae spe-1* mutants, with an altered ratio between glucans and mannoproteins, and the consequent accumulation of new mannoprotein molecules on the outer cell wall (Miret *et al.*, 1992). Also, examination of *S. cerevisiae sla2* and *act1-1* mutant cells has revealed aberrant morphology of the cell wall and septum due to defects in the actin cytoskeleton, similar to that observed in *H. polymorpha* (Mulholland *et al.*, 1997). A clumpy phenotype and an increased resistance to lytic enzymes have also been reported in *S. cerevisiae* vanadate-resistant mutants with altered secretion (Ballou *et al.*, 1991; Kanik-Ennulat *et al.*, 1995). Intriguingly, the metal-resistance of these mutants seems to arise from mutations that lead to different glycosylation phenotypes, and is inversely correlated to the extent of outer-chain elongation. Therefore, the aberrant appearance of the cell wall and the defects in cellular surface growth caused by vanadate in *H. polymorpha* could be linked to defects in secretion affecting the cell wall and plasma membrane architecture. To this extent the kinetics of ExG activity during growth on, and recovery from, vanadate is quite suggestive. Although the role of ExG is not fully understood, this enzyme is thought to be involved in cell wall metabolism and in the rearrangement of wall glucan (Sullivan *et al.*, 1991). This increased secretion of ExG during VGYNB culture conditions could thus be due to the need to soften the rigid cell wall, thus allowing the insertion of new wall material. The further increase in ExG activity during the first 60 min of recovery, concomitant with the peak in CPY activity and with the increase in electron-dense structures, would permit this observed general reorganization of the cell wall components.

Another metabolic process strongly influenced by vanadate in *H. polymorpha* is vacuolar proteolytic activity, which doubled in VGYNB and initially continued to increase upon the return to vanadate-free medium, reaching a peak 60 min after the transfer. These higher levels of CPY activity were associated with the presence of electron-dense material inside the vacuoles and with a doubling in the appearance of vacuolar finger-like protrusions. This feature, previously observed in *P. pastoris* cells undergoing microautophagy, was initially accompanied by a significant reduction of vacuolar volume. Thus, the involvement of CPY in the degradation of proteins and peptides following adaptation to changing or limiting nutritional conditions, together with the observed ultrastructural modifications, suggest the activation of an autophagic mechanism. Autophagy has been described in *S. cerevisiae* cells which, under nutrient depletion, degrade part of their cytoplasm to supply required nutrients (Takeshige *et al.*, 1992), and the vacuole has been shown to be an important site for the degradation of cytosolic components during nutrient stress in the methylotrophic yeast *P. pastoris* (Tuttle & Dunn, 1995). As the presence of vanadate in the growth medium could inhibit nutrient utilization, such inhibition could in part be responsible for the low growth rate observed in VGYNB and cause the activation of an autophagic mechanism. Upon transfer to vanadate-free medium, the cells would continue to experience this inhibition (as shown by the delay in the resumption of growth) due to the presence of vanadate or other forms of the metal ion complexed with the cell wall polymers and/or within the cell, as has already been seen in *H. polymorpha* (Zoroddu *et al.*, 1991). This thus implies that, to resume normal growth, cells must undergo a process of elimination of these vanadium-containing compounds. Also, the elimination/resorption of cell wall or plasma membrane that has been incorrectly assembled during exponential growth on VGYNB may be necessary for growth resumption. Thus, a certain degree of autophagy would be induced by vanadate-dependent inhibition of nutrient utilization, whilst the dramatic ultrastructural modifications observed upon recovery from vanadate would be part of the process of elimination/resorption of aberrant cellular structures and/or sites involved in vanadate accumulation. Therefore, vacuoles are involved not only in vanadate detoxification during growth on VGYNB (Mannazzu *et al.*, 1997), but also in the normalization of ultrastructure and metabolic functions during recovery from vanadate.

ACKNOWLEDGEMENTS

We would like to thank Dr Chris Berrie for critical appraisal of the manuscript and Dr Jesus Zueco for providing the anti-invertase antibody.

REFERENCES

- Aibara, S., Hayashi, R. & Hata, T. (1971). Physical and chemical properties of yeast proteinase. *Agric Biol Chem* 35, 658–666.
- Ballou, L., Hitzeman, R. A., Lewis, M. S. & Ballou, C. E. (1991).

- Vanadate-resistant yeast mutants are defective in protein glycosylation. *Proc Natl Acad Sci USA* **88**, 3209–3212.
- Bowman, B. J. (1983).** Vanadate uptake in *Neurospora crassa* occurs via phosphate transport system II. *J Bacteriol* **153**, 286–291.
- Bradford, M. M. (1976).** A rapid and sensitive method for the quantitation of microgram quantities of protein utilizing the principle of protein–dye binding. *Anal Biochem* **72**, 248–254.
- Brown, D. & Gordon, J. (1984).** The stimulation of pp60v-src kinase activity by vanadate in intact cells accompanies a new phosphorylation state of the enzyme. *J Biol Chem* **259**, 9580–9586.
- Cantley, L. C., Resh, M. D. & Guidotti, G. (1978).** Vanadate inhibits the red cell (Na, K) ATPase from the cytoplasmic side. *Nature* **272**, 552–554.
- Catalan, R. E., Martinez, A. M. & Aragones, M. D. (1980).** Effects of vanadate on the cyclic AMP-protein kinase system in rat liver. *Biochem Biophys Res Commun* **96**, 672–677.
- Chambers, R. S. & Sullivan, P. A. (1993).** Expression of the exoglucanase gene in yeast and hyphal forms of *Candida albicans*. *FEMS Microbiol Lett* **111**, 63–68.
- Chasteen, N. D. (1984).** The biochemistry of vanadium. *Struct Bonding* **53**, 104–138.
- Crans, D. C., Mahroof-Tahir, M. & Keramidis, A. D. (1995).** Vanadium chemistry and biochemistry of relevance for use of vanadium compounds as antidiabetic agents. *Mol Cell Biochem* **153**, 17–24.
- Foulkes, J. G., Erikson, E. & Erikson, R. (1983).** Separation of multiple phosphotyrosyl- and phosphoseroyl-protein phosphatases from chicken brain. *J Biol Chem* **258**, 431–438.
- Goldstein, A. & Lampen, J. O. (1975).** β -D-Fructofuranoside fructohydrolase from yeast. *Methods Enzymol* **42**, 505–511.
- Harsay, E. & Bretscher, A. (1995).** Parallel secretory pathways to the cell surface in yeast. *J Cell Biol* **131**, 297–310.
- Hatch, M., Freil, R. W., Goldner, A. W. & Earnest, D. L. (1983).** Vanadium ion stimulation of chloride secretion by rabbit colonic epithelium. *Biochim Biophys Acta* **732**, 699–704.
- Kanik-Ennulat, C., Montalvo, E. & Neff, N. (1995).** Sodium orthovanadate-resistant mutants of *Saccharomyces cerevisiae* show defects in Golgi-mediated protein glycosylation, sporulation and detergent resistance. *Genetics* **140**, 933–943.
- Karlish, S. J. D., Beaugé, L. A. & Glynn, I. M. (1979).** Vanadate inhibits (Na⁺ + K⁺)ATPase by blocking a conformational change of the unphosphorylated form. *Nature* **282**, 333–335.
- Karlund, J. (1985).** Transformation of cells by an inhibitor of phosphatases acting on phosphotyrosine proteins. *Cell* **41**, 707–717.
- Lew, D. J. & Simon, S. M. (1991).** Characterization of constitutive exocytosis in the yeast *Saccharomyces cerevisiae*. *J Membr Biol* **123**, 261–268.
- Lindquist, R. N., Lynn, J. L. & Lienhard, G. E. (1973).** Possible transition-state analogs for ribonuclease. The complexes of uridine with oxovanadium (IV) ion and vanadium (V) ion. *J Am Chem Soc* **95**, 8762–8768.
- Mannazzu, I., Guerra, E., Strabbioli, R., Masia, A., Maestrale, G. B., Zoroddu, M. A. & Fatichenti, F. (1997).** Vanadium affects vacuolation and phosphate metabolism in *Hansenula polymorpha*. *FEMS Microbiol Lett* **147**, 23–28.
- Miret, J. J., Solari, A. J., Barderi, A. P. & Goldemberg, S. H. (1992).** Polyamines and cell wall organization in *Saccharomyces cerevisiae*. *Yeast* **8**, 1033–1041.
- Mulholland, J., Preuss, D., Moon, A., Wong, A., Drubin, D. & Botstein, D. (1994).** Ultrastructure of the yeast actin cytoskeleton and its association with the plasma membrane. *J Cell Biol* **125**, 381–391.
- Mulholland, J., Wesp, A., Riezman, H. & Botstein, D. (1997).** Yeast actin cytoskeleton mutants accumulate a new class of Golgi-derived secretory vesicles. *Mol Biol Cell* **8**, 1481–1499.
- Novick, P., Field, C. & Schekman, R. (1980).** Identification of 23 complementation groups required for post-translational events in the yeast secretory pathway. *Cell* **21**, 205–215.
- Preuss, D., Mulholland, J., Kaiser, C. A., Orlean, P., Albright, C., Rose, M. D., Robbins, P. W. & Botstein, D. (1991).** Structure of the yeast endoplasmic reticulum: localization of ER proteins using immunofluorescence and immunoelectron microscopy. *Yeast* **7**, 891–911.
- Rambourg, A., Clermont, Y., Jackson, C. L. & Kepes, F. (1994).** Ultrastructural modifications of vesicular and Golgi element in the *Saccharomyces cerevisiae* *sec21* mutant at permissive and non-permissive temperatures. *Anat Rec* **240**, 32–41.
- Santos, T., Del Rey, F., Conde, J., Villanueva, J. R. & Nombela, C. (1979).** *Saccharomyces cerevisiae* mutants defective in exo-1,3- β -glucanase production. *J Bacteriol* **139**, 333–338.
- Smith, J. (1983).** Vanadium ions stimulate DNA synthesis in Swiss mouse 3T3 and 3T6 cells. *Proc Natl Acad Sci USA* **80**, 6162–6166.
- Sullivan, P. A., Emerson, G. W., Broughton, M. J. & Stubbs, H. J. (1991).** Transglucosylation catalysed by the exo- β -glucanase of *Candida albicans*. In *Candida and Candidamycosis*, pp. 35–38. Edited by E. Tumbay, H. P. R. Seeliger & O. Ang. New York: Plenum.
- Takehige, K., Baba, M., Tsuboi, S., Noda, T. & Oshumi, Y. (1992).** Autophagy in yeast demonstrated with proteinase-deficient mutants and condition for its induction. *J Cell Biol* **119**, 301–311.
- Tuttle, D. L. & Dunn, W. A., Jr (1995).** Divergent modes of autophagy in the methylotrophic yeast *Pichia pastoris*. *J Cell Sci* **108**, 25–35.
- Wach, A. & Graber, P. (1991).** The plasma membrane H⁺-ATPase from yeast. Effects of pH, vanadate and erythrosine B on ATP hydrolysis and ATP binding. *Eur J Biochem* **201**, 91–97.
- Weibel, E. R. (1979).** *Stereological Methods: Practical Methods for Biological Morphometry*, vol. 1. London: Academic Press.
- Willsky, G. R. (1990).** Vanadium in the biosphere. In *Vanadium in Biological Systems*, pp. 1–24. Edited by N. D. Chasteen. Dordrecht: Kluwer.
- Willsky, G. R., White, D. A. & McCabe, B. C. (1984).** Metabolism of added orthovanadate to vanadyl and high-molecular-weight vanadate by *Saccharomyces cerevisiae*. *J Biol Chem* **259**, 13273–13281.
- Zoroddu, M. A., Bonomo, R. P., Di Bilio, A. J., Berardi, E. & Meloni, M. G. (1991).** EPR study on vanadyl and vanadate ion retention by a thermotolerant yeast. *J Inorg Biochem* **43**, 731–738.

Received 2 March 1998; revised 7 May 1998; accepted 11 May 1998.